MPE — Volume 2, pp. 219-231
Reprints available directly from the publisher
Photocopying permitted by license only

A SELF-CONSISTENT NUMERICAL METHOD FOR SIMULATION OF QUANTUM TRANSPORT IN HIGH ELECTRON MOBILITY TRANSISTOR; PART II: THE FULL QUANTUM TRANSPORT

R. KHOIE

Department of Electrical and Computer Engineering, University of Nevada, Las Vegas, Las Vegas, NV 89154

(Received 24, March, 1995)

In Part I of this paper we reported a *self-consistent Boltzmann-Schrödinger-Poisson* simulator for HEMT in which only electrons in the *first subband* were assumed to be quantized with their motion restricted to 2 dimensions. In that model, the electrons in the second and higher subbands were treated as bulk system behaving as a 3 dimensional electron gas. In Part II of this paper, we extend our simulator to a *self-consistent full-quantum* model in which the electrons in the *second subband* are also treated as quantized 2 dimensional gas. In this model, we consider the electrons in the lowest *two subbands* to be in the quantum well forming the 2-dimensional electron gas, and the electrons in the third and higher subbands to behave as bulk electrons with no restrictions in their motion. We have further incorporated an additional self-consistency by calculating the field-dependent, energy-dependent scattering rates due to ionized impurities and polar optical phonons. The two higher moments of Boltzmann transport equation are numerically solved for the two lowest subbands and the bulk system; six transport equations, four for the two subbands and two for the bulk system. The Schrödinger and Poisson equations are also solved self-consistently. The wavefunctions obtained are used to calculate the ionized impurity scattering and the polar optical phonon scattering rates. The rates of transfer of electrons and their energies to and from each subband are calculated from these intersubband and intrasubband scattering rates.

KEYWORDS: *Numerical; transport; HEMT; quantum; self-consistent; scattering*

1. INTRODUCTION

At 77°K, 98 percent of electrons in the quantum well of a HEMT device reside in the lowest subband whereas at 300°K, the population of electrons residing in the lowest subband reduces to 68 percent [1]. In fact, at 300°K close to 20 percent of electrons in the quantum well reside in the second subband with their motion restricted to two dimensions. In Part I of this paper, we presented a self-consistent Boltzmann-Schrödinger-Poisson simulator for HEMT [2], in which the quantization of electrons in the quantum well was taken into account. In that model, however, we assumed that only the electrons in the first subband were quantized, and that the electrons in the second and higher subbands behave as bulk electrons with no dimensional restriction in their motion. This assumption, particularly at 300°K, in light of the fact that only 68 percent of electrons reside in the first subband, becomes questionable.

In Part II of this paper, we extend our One Subband Boltzmann-Poisson-Schrödinger (**OS-BPS**) simulator to a Full Quantum Boltzmann-Poisson-Schrödinger (**FQ-BPS**) model. In this model, we consider the electrons in the lowest *two subbands* to be in the

quantum well forming the 2-dimensional electron gas, and the electrons in the third and higher subbands to behave as bulk electrons with no restrictions in their motion. Taking the quantization of electrons in the third subband into consideration, as the notion of "Full Quantum" implies, would not significantly improve the accuracy of the model, because of relatively small population of electrons in that subband, or at least, the computational effort required is not justified for the added accuracy of the results.

In our FQ-BPS model, we solve Boltzmann, Poisson, and Schrödinger equations for the first subband, second subband, and the bulk system. An additional self-consistency has been added by calculating the intersubband and intrasubband scattering due to polar optical phonon and ionized impurity scattering mechanisms [3]. The rates of transfer of electrons and their energies to and from each subband are calculated from the intersubband and intrasubband scattering rates, and are used in the in a self-consistent manner in the Boltzmann-Poisson-Schrödinger simulator.

2. FULL QUANTUM TRANSPORT

2.1. Boltzmann-Poisson-Schrödinger System

In the full quantum transport model the Poisson and Schrödinger equations are written as before [2]:

$$\frac{\partial^2 V}{\partial x^2} + \frac{\partial^2 V}{\partial y^2} = -\frac{q}{\epsilon}[N_D(x, y) - n(x, y)] \tag{1}$$

and

$$-\frac{\hbar^2}{2m^*}\frac{d^2\psi_i(x)}{dx^2} - qV(x, y)\psi_i(x) = E_i\psi_i(x) \tag{2}$$

where q is the electronic charge, ϵ the dielectric constant, n the total electron concentration, N_D the doping level, m^* is the electron effective mass, $V(x, y)$ the electrostatic potential, and ψ_i the wavefunction corresponding to the eigenenergy E_i for the i-th subband.

For FQ-BPS model, the two higher moments of Boltzmann transport equation require considerable modifications. The particle conservation, Eq. (3), and the energy conservation Eq. (4) for the first two subbands of the quantum well are written as:

$$\frac{\partial(n_i(x, t))}{\partial t} = \nabla\cdot(-\mu_i n_i(x, t)\nabla V(x) + \nabla(D_i n_i(x, t))) + \sum_{j\neq i}\left(\frac{n_j - n_{oj}}{\tau_{ji}}\right) - \sum_{j\neq i}\left(\frac{n_i - n_{oi}}{\tau_{ij}}\right) \quad i = 1, 2 \tag{3}$$

$$\frac{\partial(n_i(x,t)E_i(x,t))}{\partial t} = -J\cdot\nabla V(x) + \nabla\cdot(-\mu_{E,i}n_i(x,t)E_i(x,t)\nabla V(x) + \nabla(D_{E,i}n_i(x,t)E_i(x,t)))$$

$$+ \sum_{j\neq i}\left(\frac{n_jE_j - n_{jo}E_{oj}}{\tau_{E,ji}}\right) - \sum_{j\neq i}\left(\frac{n_iE_i - n_{io}E_{io}}{\tau_{E,ij}}\right) - \sum_{j\neq i}\left(\frac{n_j - n_{oj}}{\tau_{ji}}\right)\hbar\omega_0 \quad i = 1,2 \tag{4}$$

In the above equations $i = 1, 2$ refers to the first and second subbands, respectively. n is the electron concentration, J is the electron current density, q is the electronic charge, μ_i is the mobility, D_i is diffusivity, $\mu_{E,i}$ is flux mobility, $D_{E,i}$ is the flux diffusivity, E is the average electron energy, τ_{ij} is particle relaxation time, $\tau_{E,ij}$ is energy relaxation time for particles moving from subband i to subband j, and $\hbar\omega_0$ is the polar optical phonon energy. ∇ represents $\partial/\partial y$ in the one-dimensional quantum well. The first summation term $(\sum_{j\neq i}(n_j - n_{oj}/\tau_{ji}))$ in Eq. (3), accounts for the particles moving from subband j to subband i, and the second summation term $(-\sum_{j\neq i}(n_i - n_{oi}/\tau_{ij}))$ in Eq. (3), accounts for the particles moving from subband i to subband j. The first summation term $(\sum_{j\neq i}(n_jE_j - n_{jo}E_{oj}/\tau_{E,ji}))$ in Eq. (4) accounts for the energy gained due to the movement of particles from subband j to subband i, and the second summation term $(-\sum_{j\neq i}(n_iE_i - n_{io}E_{io}/\tau_{E,ij}))$ in Eq. (4), accounts for the energy loss due to the movement of particles from subband i to subband j. Finally, the last summation term $(-\sum_{j\neq i}(n_j - n_{oj}/\tau_{ji}))\hbar\omega_0)$, in Eq. (4) includes the effect of the loss of energy by the electron to the polar optical phonons.

In the bulk (electrons in the third and higher subbands), particle conservation, and energy conservation equations are:

$$\frac{\partial n}{\partial t} = \nabla\cdot(-\mu n\nabla V + \nabla(Dn)) + G_i \quad i = 1,2 \tag{5}$$

$$\frac{\partial(nE)}{\partial t} = -J\cdot\nabla V - nB + \nabla\cdot\alpha(-\mu nE\nabla V + \nabla(DnE)) + F_i \quad i = 1,2 \tag{6}$$

where B is the energy dissipation factor, α is a constant relating μ to μ_E and D to D_E. ∇ represents $(\partial/\partial x, \partial/\partial y)$ in the two-dimensional bulk. The term G_i is the generation-like term that takes into account the transfer of electrons between the bulk and the first (i = 1) and second (i = 2) subbands. The term F_i is a similar term that takes the rate of energy transfer between the bulk and the two subbands into consideration [4].

2.2. Self-consistent Scattering Rates

The eigenfunctions obtained from the Boltzmann-Poisson-Schrödinger simulator are used to calculate the ionized impurity scattering and the polar optical phonon scattering rates for the two lowest subbands in the quantum well. The rates of transfer of electrons and their energies to and from each subband are calculated from these intersubband and intrasubband scattering rates. For independent scattering mechanisms, the total scattering rate (the total scattering rate represents the probability per unit time that an electron with a state wave vector $\mathbf{K_1}$ is scattered into a state with a wave vector $\mathbf{K_2}$) is defined by [5]:

$$\frac{1}{\tau_{tot}^{all}} = \frac{1}{\tau_{tot}^{I}} + \frac{1}{\tau_{tot}^{pop}} = \sum S(\mathbf{K_1}, \mathbf{K_2}) \tag{7}$$

where the superscript I denotes the impurity scattering, and *pop* denotes the polar optical phonon scattering, τ is the relaxation time, and $S(\mathbf{K_1}, \mathbf{K_2})$ is the probability of an electron being scattered. The polar optical phonon scattering rate is given by [1]:

$$S_{mn}^{pop} = \frac{e^2\omega_0}{8\pi\epsilon_0}\left[\frac{1}{\epsilon_\infty} - \frac{1}{\epsilon_s}\right](N_q + \frac{1}{2} \pm \frac{1}{2}) \times \int \frac{H_{mn}(Q)}{Q}\delta(E(\mathbf{k_2}) - \mathrm{E}(\mathbf{k_1}) \pm \hbar\omega_0)\mathrm{d}\mathbf{k_2} \tag{8}$$

where, ϵ_∞ and ϵ_s are the optical and static dielectric constant, $\hbar\omega_0$ is the polar optical phonon energy, Q is the phonon wave-vector component parallel to the interface, $\mathbf{k_1}$ and $\mathbf{k_2}$ denote the initial and final state wave vectors. N_q is the phonon occupation number, and $E(\mathbf{k_1})$ and $E(\mathbf{k_2})$ are the initial and final state energies. $H_{mn}(Q)$'s are the multisubband coupling coefficients and are given by [2]:

$$H_{mn}(Q) = \int\int \psi_{mn}(z_1)\psi_{mn}(z_2)exp(-Q|z_1 - z_2|)dz_1dz_2 \tag{9}$$

where $\psi_{mn}(z) = \psi_m(z)\psi_n(z)$ are obtained from the eigenfunctions of Schrödinger equation. The ionized impurity scattering rate is given by [1]:

$$S_{mn}^{imp} = \frac{1}{2\pi\hbar}\int |M_{mn}(Q)|^2\delta(E(\mathbf{k_2}) - \mathrm{E}(\mathbf{k_1}))\mathrm{d}\mathbf{k_2} \tag{10}$$

The matrix elements $M_{mn}(Q)$ account for the electron-impurity interactions. For more details of the modeling of scattering rates see [3].

2.3. Numerical Methods

As shown in the flow chart of Fig. 1, we begin the numerical simulation with an initial guess for the electron densities in the bulk and in the quantum well. Then, we start the iterative process by solving the Poisson and Schrödinger equations self-consistently, from which we obtain the electrostatic potential V, the eigenvalues E_i, and the wavefunctions ψ_i. The scattering rates are calculated next, using the eigenvalues and wavefunctions obtained. The mobilities and the coupling terms in the Boltzmann equations are derived from these scattering rates. Finally we solve the two moments of Boltzmann equation and obtain the $I_D - V_D$ characteristics of the device. For details of the numerical discretization of the system of differential equations and the numerical instability problems see Part I of this paper [2] and also [6] and [7].

3. RESULTS

The structure of the HEMT device used in our simulations is that reported in Part I of this paper. The variations of the drain current with the drain voltage are calculated under three

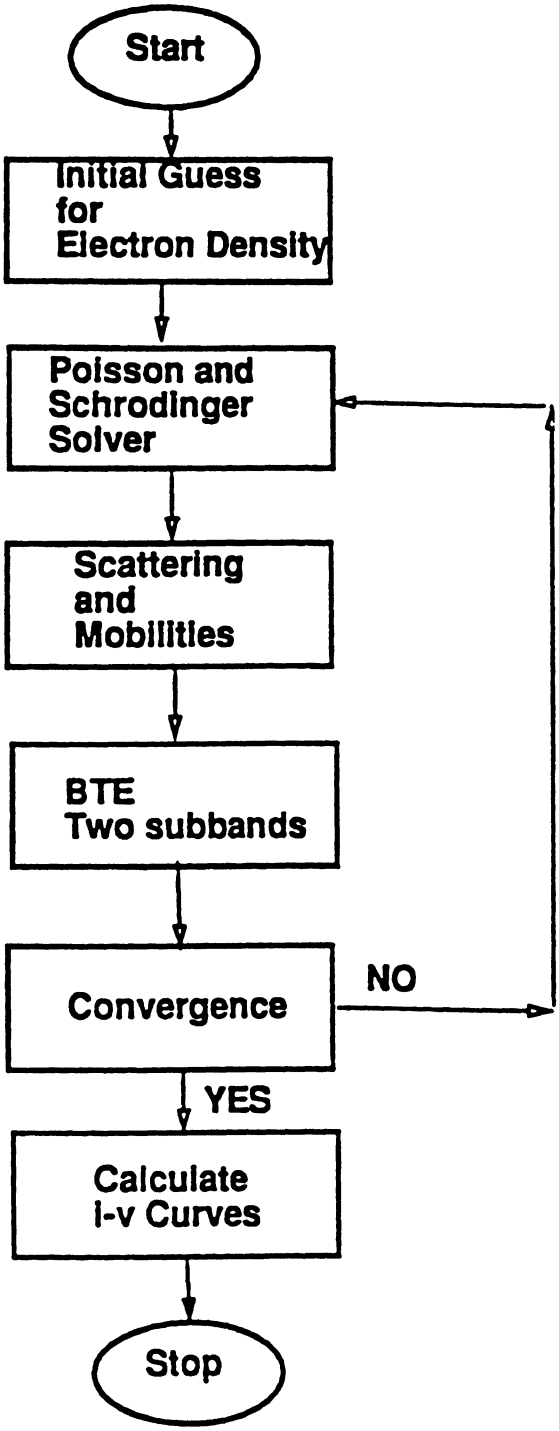

Figure 1 The Flow chart of the numerical iteration in FQ-BPS model.

different gate biasing conditions: V_g = 0.45 V, 0.5 V, and 0.7 V. Fig. 2 shows the $I_D - V_D$ characteristics of the device along with those calculated by our One Subband Boltzmann-Poisson-Schrödinger (**OS-BPS**) simulator [2]. In both cases, the slopes of the $I_D - V_D$ curves decrease as drain voltage increases, but the Full Quantum Boltzmann-Poisson-Schrödinger solver (**FQ-BPS**) model predicts lower drain currents. The reason is that with the scattering rates included in the model, the electron density in the quantum well decreases, which results in lower drain currents. The overestimation of the drain current by the (OS-BPS) model can be seen from the $I_D - V_D$ characteristics of Fig. 2. In FQ-BPS model, when a gate bias of 0.7 V is applied, the slope of the drain current decreases substantially above a drain voltage of 0.8 V, which is the saturation region, whereas the drain current obtained from OS-BPS model still has a sharp slope as the drain voltage is

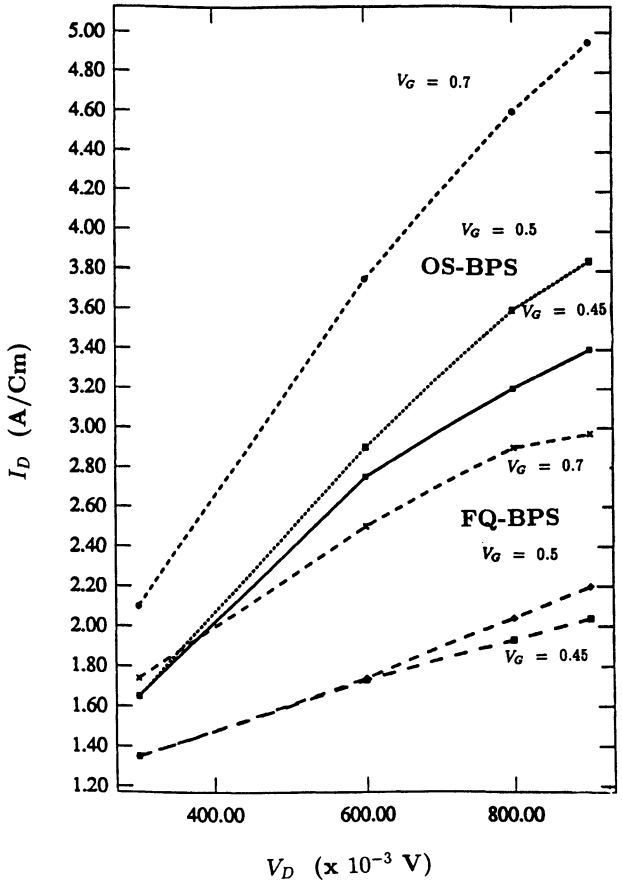

Figure 2 $I_D - V_D$ characteristics: (OS-BPS) are the results from the one subband Boltzmann-Poisson-Schrödinger solver, and (FQ-BPS) are the results from the full quantum Boltzmann-Poisson-Schrödinger simulator.

increased, and the onset of saturation occurs at around 1.2 V. Therefore, the FQ-BPS model shows that the device goes into saturation at a lower drain voltage than the value predicted by OS-BPS model.

Fig. 3 shows the variations of the electrostatic potential with a gate voltage of 0.7 V, and drain voltages of 0.5 V, and 1.35 V. Under these biasing conditions, the electron concentrations in the bulk, first, and second subbands are shown in Figs. 4 through 6. The concentration of the electrons in the quantum well (for the lowest two subbands) is obtained by multiplying the probability density $\psi_i(x)^2$, (for $i = 1, 2$), by the electron sheet density. The most important observation that can be made is that at room temperature, 72 percent of electrons reside in the first subband and 26 percent reside in the second

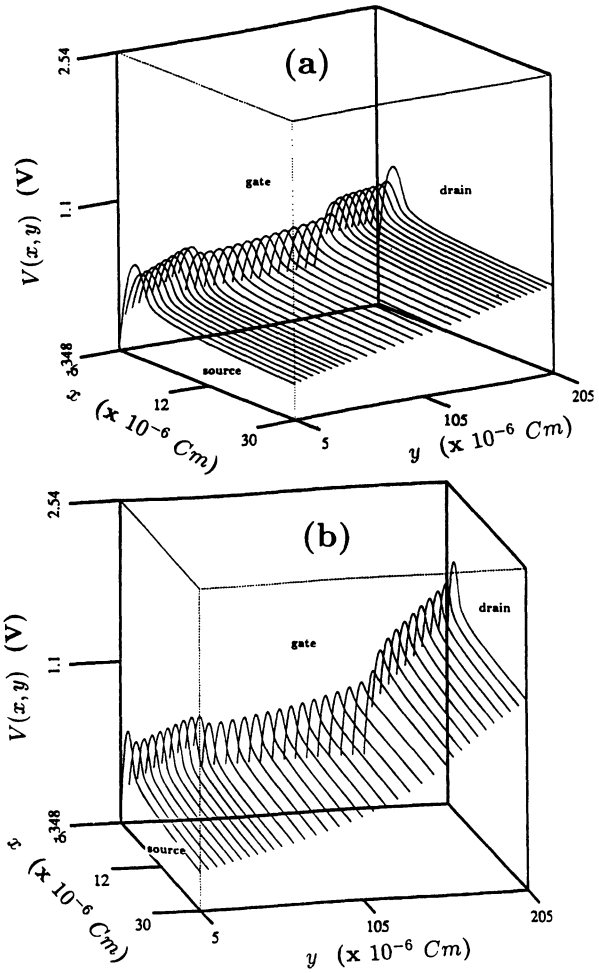

Figure 3 Electrostatic potential with a gate voltage of 0.7V and a) a drain voltage of 0.5V, b) a drain voltage of 1.35V.

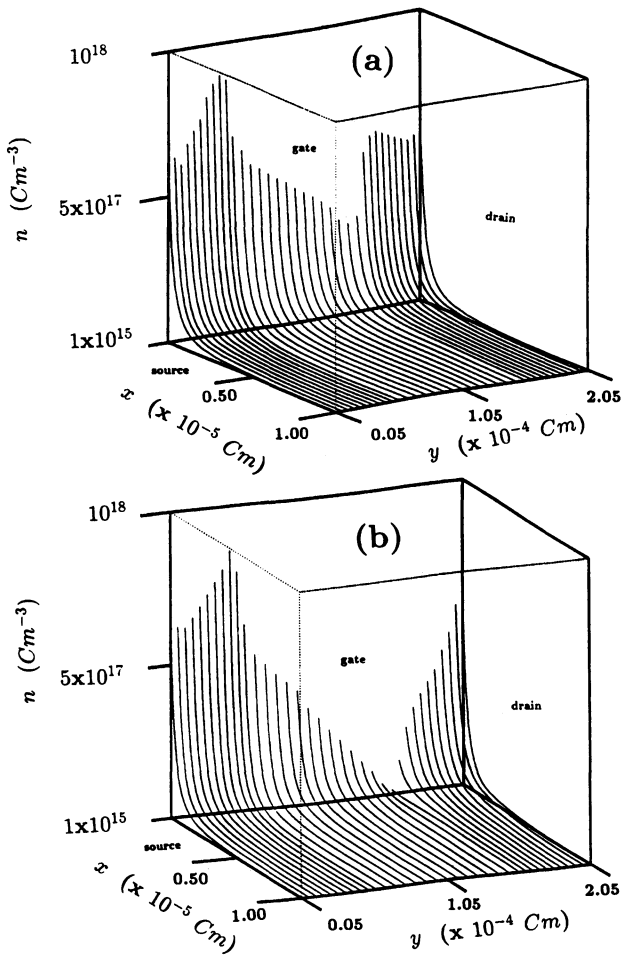

Figure 4 Electron concentration in the bulk with a gate voltage of 0.7V and a) a drain voltage of 0.5V, where we observe the pinch-off, b) a drain voltage of 1.35V.

subband. These results agree very well with those calculated by the Monte Carlo simulator reported by Yokoyama and Hess [1] who concluded that the population of electrons in the first and second subband are 68 percent, and 20 percent, respectively. It is therefore concluded that full quantum modeling of HEMT must include the quantization of electrons in the second subband, as well as the coupling terms between and amongst the subbands.

The multisubband coupling coefficients, $H_{1n}(Q)$, (From Eq. (9)), calculated by the FQ-BPS model are depicted in Fig. (7a), and those calculated by the Monte Carlo simulator of Yokoyama and Hess [1] are shown in Fig. (7b). The agreement between the two sets of data is excellent. The FQ-BPS simulator, however, uses substantially less computation time than the Monte Carlo simulator.

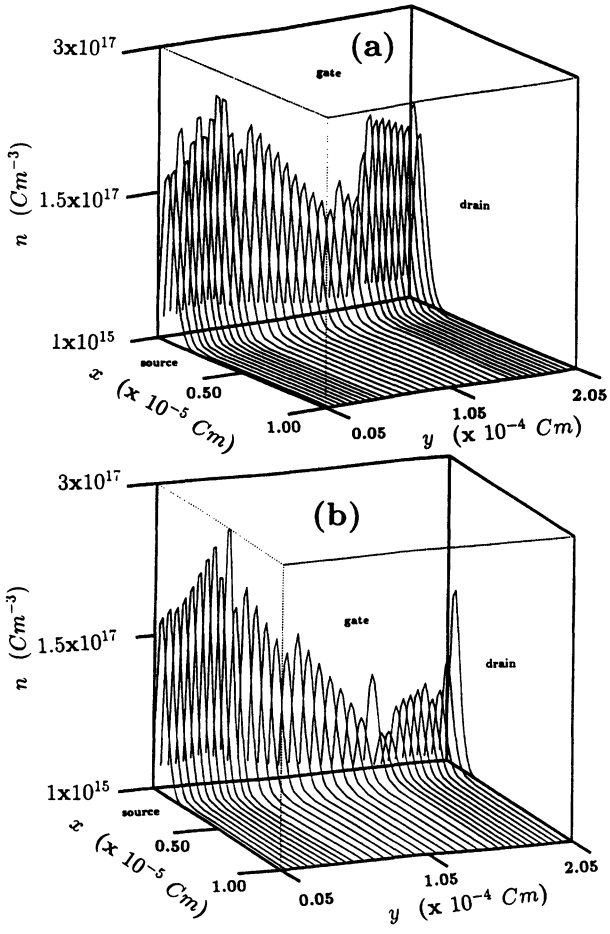

Figure 5 Electron concentration in the quantum well for the first subband with a gate voltage of 0.7V and a) a drain voltage of 0.5V b) a drain voltage of 1.35V. The concentration of the electrons in the quantum well is obtained by multiplying the probability density $\psi_1(x)^2$ by the electron sheet density.

The drain current as a function of the gate voltage under a constant drain voltage of 1.0 V is shown in Fig. 8(a), along with the results from our OS-BPS model. Fig. 8(b) shows the total charge, Q, in channel as a function of the applied gate voltage, V_g, along with the result from the OS-BPS model. The values of transconductance under various gate voltages are shown in Fig. 9(a), compared to the results of our OS-BPS model. It can be seen that with our FQ-BPS model, as it has been reported by Widiger, [8] Loret [9], and Kizilyalli [10], the transconductance increases with the gate voltage at low gate voltages, and then decreases as the gate voltage is further increased. This effect is not seen in the OS-BPS results, where the transconductance decreases linearly. Similar patterns are observed in Figs. 9(b) and 9(c), where the gate capacitance and unity-gain frequency are presented, respectively. With the FQ-BPS model we obtain smaller drain currents and

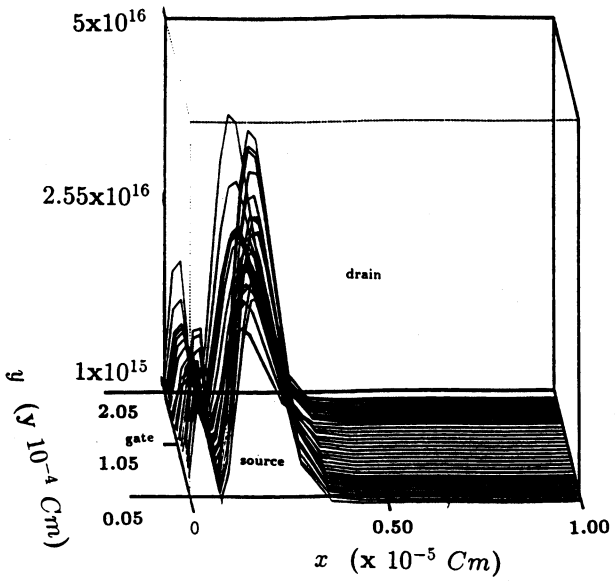

Figure 6 Electron concentration in the quantum well for the second subband with a gate voltage of 0.7V and a drain voltage of 0.5V (at a different angle, where we see the two peaks due to ψ_2).

smaller transconductances compared to the OS-BPS model. For example, at a gate bias of about 0.625 V, FQ-BPS predicts a transconductance of 316 mS/mm, compared to 520 mS/mm predicted by OS-BPS model; a gate capacitance of 17.68 pF/cm, compared to 21 pF/cm; and a unity-gain frequency of 28.44 GHz, compared to 39 GHz.

4. CONCLUSIONS

A full-quantum Boltzmann-Poisson-Schrödinger simulator, (FQ-BPS), with two-subband quantum transport model has been developed. In this model we have considered the electrons in the lowest *two subbands* to be in the quantum well forming the 2-dimensional electron gas, and the electrons in the third and higher subbands to behave as bulk electrons with no restrictions in their motion. We have further incorporated an additional self-consistency by calculating the field-dependent, energy-dependent scattering rates due to ionized impurities and polar optical phonons.

The results of the polar optical phonon and ionized impurity scattering rates from our FQ-BPS are in very good agreement with those calculated by significantly more computation intensive Monte Carlo simulators reported by others. [1]

From the results of the $I_D - V_D$ characteristics of these devices it has been found that at a given gate voltage, the FQ-BPS model predicts lower transconductance and drain currents than the OS-BPS. The overestimation by OS-BPS model is mainly due to the scattering rates that were not included in the quantum well. Also, with the FQ-BPS model we observe the well known pattern reported by [8]–[10], in which the transconductance increases with the gate voltage at low gate bias, and as the gate bias is increased further, the transconductance starts to decrease. This pattern was not seen in the OS-BPS results.

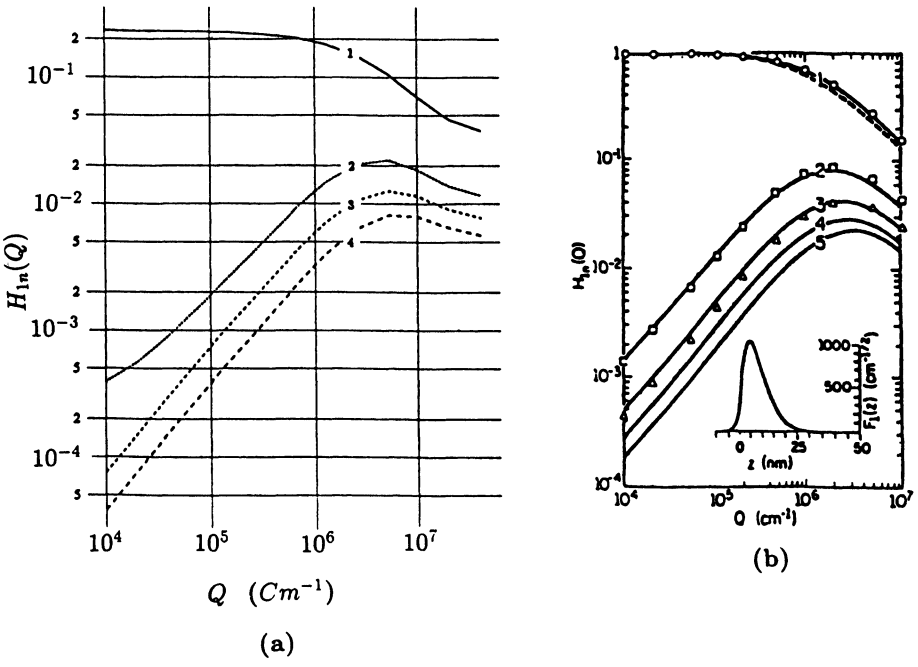

Figure 7 Multisubband coupling coefficients $H_{1n}(Q)$, for transfer of electrons from the first subband to the other subbands as a function of Q, the phonon wave vector, calculated by: (a) FQ-BPS model, and (b) Monte Carlo simulator reported by Yokoyama and Hess [1].

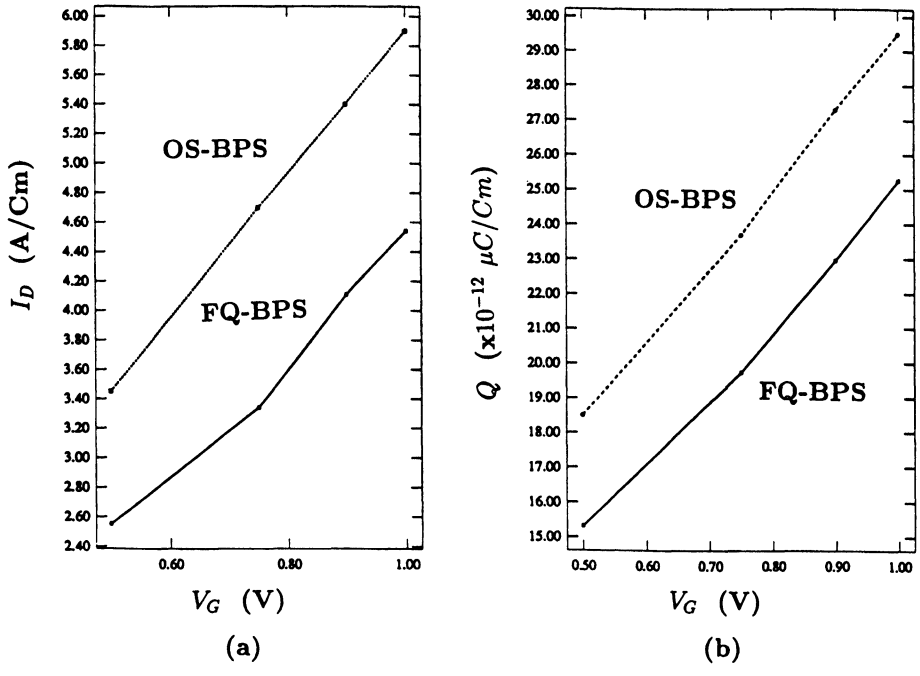

Figure 8 a) $I_D - V_G$, (b) $Q - V_G$ characteristics under a drain voltage of 1.0 V. (OS-BPS) are the results from the one subband Boltzmann-Poisson-Schrödinger solver, and (FQ-BPS) are the results from the full quantum Boltzmann-Poisson-Schrödinger model.

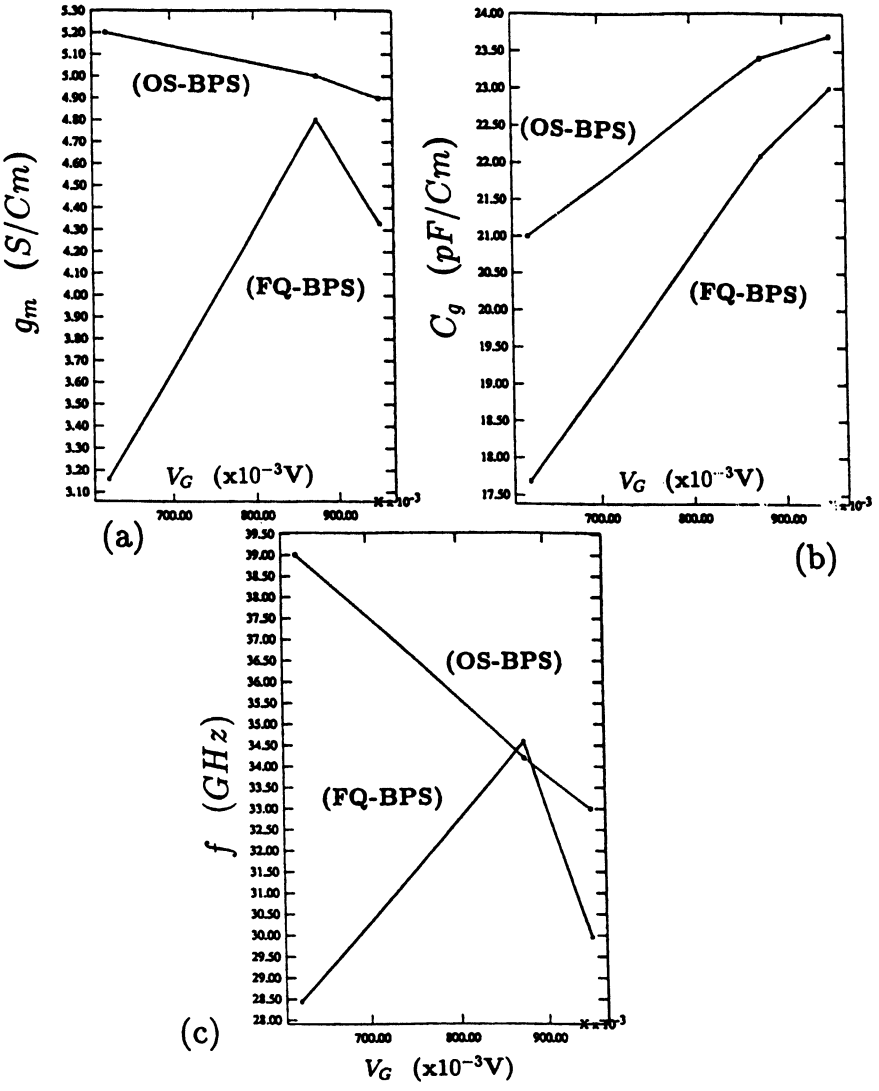

Figure 9 a) Transconductance, (b) gate capacitance, and (c) unity gain frequency under a drain voltage of 1.0 V. (OS-BPS) are the results from the one subband Boltzmann-Poisson-Schrödinger solver, and (FQ-BPS) are the results from the full quantum Boltzmann-Poisson-Schrödinger model.

We therefore conclude that the quantization of the electrons in the second subband of the quantum well is essential in any numerical simulation of HEMT, and these electrons must not be considered as bulk. Treating these electrons as bulk indeed introduces error in the results in the form of overestimation of the drain current, the channel conductance, and transconductance as well as unity-gain frequency.

The results produced by our FQ-BPS model suggest the significance of incorporating the quantum transport of the electrons in the *second subband*. It is, however, believed that

taking the quantization of electrons in the *third and higher subbands* into consideration, as the notion of "Full Quantum" implies, would not significantly improve the accuracy of the model, because of relatively small population of electrons in those subbands, or at least the computational effort required is not justified for the added accuracy of the results.

References

1 K. Yokoyama and K. Hess, "Monte Carlo Study of the Electronic Transport in $Al_{1-x}Ga_xAs/GaAs$ Single-Well Heterostructure", *Physical Review B*, Vol. 33, no. 8, pp. 5595–5606, 1986.

2 R. Khoie, "A Self-consistent Numerical Method for Simulation of Quantum Transport in High Electron Mobility Transistor; Part I: The Boltzmann-Poisson-Schrödinger Solver", *Elsewhere in this Publication*, 1996.

3 H. Arman, and R. Khoie, "A Self-Consistent Multisubband Model for Calculation of Scattering Rates in Quantum Well Structures", *National Center for Computational Electronics, Proceedings of the International Workshop on Computational Electronics*, edited by: K. Hess, U. Ravaioli, and R. Dutton, *Beckman Institute, University of Illinois at Urbana-Champaign*, pp. 175–179, 1992.

4 R. Khoie and H. Arman, "A Two-Subband Self-Consistent Model for High Electron Mobility Transistor Including Intersubband and Intrasubband Scattering Mechanisms", *National Center for Computational Electronics, Proceedings of the International Workshop on Computational Electronics*, edited by: K. Hess, U. Ravaioli, and R. Dutton, *Beckman Institute, University of Illinois at Urbana-Champaign*, pp. 181–184, 1992.

5 K. Hess, *Advanced Theory of Semiconductor Devices*, Englewood Cliffs, New Jersey, Prentice Hall, 1998.

6 Z. H. Ng, R. Khoie, and R. Venkat, "A Two-Dimensional Self-Consistent Numerical Model for High Electron Mobility Transistor", *IEEE Trans. on Electron Devices*, Vol. 38, No. 4, pp. 852–861, 1991.

7 Z. H. Ng, R. Khoie, and R. Venkat, "A Self-Consistent Calculation of Spatial Spreading of the Quantum Well in HEMT", *Computational Electronics, Semiconductor Transport and Device Simulation*, edited by: K. Hess, J.P. Leburton, and U. Ravaioli, Kluwer Academic, pp. 55–58, 1991.

8 D. J. Widiger, I. C. Kizilyalli, K. Hess, and J. J. Coleman, "Two-Dimensional Transient Simulation of an Idealized High Electron Mobility Transistor," *IEEE Trans. on Electron Devices*, Vol. ED-32, 1092–1102, 1985.

9 D. Loret, "Two-Dimensional Numerical Model for the High Electron Mobility Transistor," *Solid-State Electronics*, Vol. 30, pp. 1197–1203, 1987.

10 I.C. Kizilyalli, M.A. Artaki, N.J. Shah, and A. Chandra, "Scaling Properties and Short-Channel Effects in Submicrometer AlGaAs/GaAs MODFET's: A Monte Carlo Study", *IEEE Trans. Electron Devices*, vol. ED-40, pp. 234–249, 1993.

Mathematical Problems in Engineering

Special Issue on Space Dynamics

Call for Papers

Space dynamics is a very general title that can accommodate a long list of activities. This kind of research started with the study of the motion of the stars and the planets back to the origin of astronomy, and nowadays it has a large list of topics. It is possible to make a division in two main categories: astronomy and astrodynamics. By astronomy, we can relate topics that deal with the motion of the planets, natural satellites, comets, and so forth. Many important topics of research nowadays are related to those subjects. By astrodynamics, we mean topics related to spaceflight dynamics.

It means topics where a satellite, a rocket, or any kind of man-made object is travelling in space governed by the gravitational forces of celestial bodies and/or forces generated by propulsion systems that are available in those objects. Many topics are related to orbit determination, propagation, and orbital maneuvers related to those spacecrafts. Several other topics that are related to this subject are numerical methods, nonlinear dynamics, chaos, and control.

The main objective of this Special Issue is to publish topics that are under study in one of those lines. The idea is to get the most recent researches and published them in a very short time, so we can give a step in order to help scientists and engineers that work in this field to be aware of actual research. All the published papers have to be peer reviewed, but in a fast and accurate way so that the topics are not outdated by the large speed that the information flows nowadays.

Before submission authors should carefully read over the journal's Author Guidelines, which are located at http://www.hindawi.com/journals/mpe/guidelines.html. Prospective authors should submit an electronic copy of their complete manuscript through the journal Manuscript Tracking System at http://mts.hindawi.com/ according to the following timetable:

Manuscript Due	July 1, 2009
First Round of Reviews	October 1, 2009
Publication Date	January 1, 2010

Lead Guest Editor

Antonio F. Bertachini A. Prado, Instituto Nacional de Pesquisas Espaciais (INPE), São José dos Campos, 12227-010 São Paulo, Brazil; prado@dem.inpe.br

Guest Editors

Maria Cecilia Zanardi, São Paulo State University (UNESP), Guaratinguetá, 12516-410 São Paulo, Brazil; cecilia@feg.unesp.br

Tadashi Yokoyama, Universidade Estadual Paulista (UNESP), Rio Claro, 13506-900 São Paulo, Brazil; tadashi@rc.unesp.br

Silvia Maria Giuliatti Winter, São Paulo State University (UNESP), Guaratinguetá, 12516-410 São Paulo, Brazil; silvia@feg.unesp.br